COMP30027 Assignment 1 - Report

Lucas Fern (1080613)

April 11, 2021

Overall, the Naïve Bayes classifier implemented for this assignment achieved an accuracy of 75.9% on the provided training data. The accuracies within individual classes varied between 42.9% and 100%, and the individual accuracies as read from the diagonal of the confusion matrix in figure 1b are:

```
Multiclass Accuracy:
    bridge: 0.429
    childs: 0.917
    downwarddog: 0.867
    mountain: 0.867
    plank: 0.667
    seatedforwardbend: 0.444
    tree: 0.667
    trianglepose: 1.000
    warrior1: 0.800
    warrior2: 0.875
```

Question 1: Multiclass Model Evaluation

For this question both Micro and Macro-Averaging were implemented for the multiclass precision, recall, and F_1 score. All of these scores can be easily generated from a confusion matrix containing the frequencies of each classification. A visualisation of the confusion matrix from running the model on the test data is shown in figure 1a, and what is perhaps a more useful confusion matrix showing the proportions is presented alongside in figure 1b.

Calculating the Micro and Macro-Averaged statistics from the confusion matrix gives the following results:

```
Multiclass Precision (Macro-Averaged):
    0.739
Multiclass Recall (Macro-Averaged):
    0.753
Multiclass F1 Score (Macro-Averaged):
    0.746
Multiclass Precision (Micro-Averaged):
    0.759
Multiclass Recall (Micro-Averaged):
    0.759
Multiclass F1 Score (Micro-Averaged):
    0.759
```

It is clear from this output that the choice of Micro vs. Macro-Averaging makes only a very small difference in this case, with the largest difference being between the Micro and Macro-Averaged precision at 2%. It is surprising that all the micro-averaged statistics are identical, but this is simply a coincidence, and it can be seen easily from the formula for the F_1 score that when the precision and recall are identical, the F_1 score will be too:

$$F_1 = \frac{2PR}{P+R}; \qquad \text{when } P = R = \alpha; \qquad F_1 = \frac{2\alpha^2}{2\alpha} = \alpha$$

Apart from this, none of the results are unexpected. The Macro-Averaged scores appear to be slightly lower since the Micro-Averaging process considers the size of the class when averaging, whereas the Macro-Averaging process takes a non-weighted average of the precision and recall from each class. This means that classes which appear in large quantities in the test data - such as the mountain pose - are represented with larger weighting in the Micro-Averaged scores. In this example, the mountain pose class has an accuracy of 0.867, which is above the average accuracy, and therefore contributes significantly to increasing the Micro-Averaged precision and recall.

Figure 1: A visualisation of two confusion matrices for the model's classification of the testing data.

(a) Using frequencies.

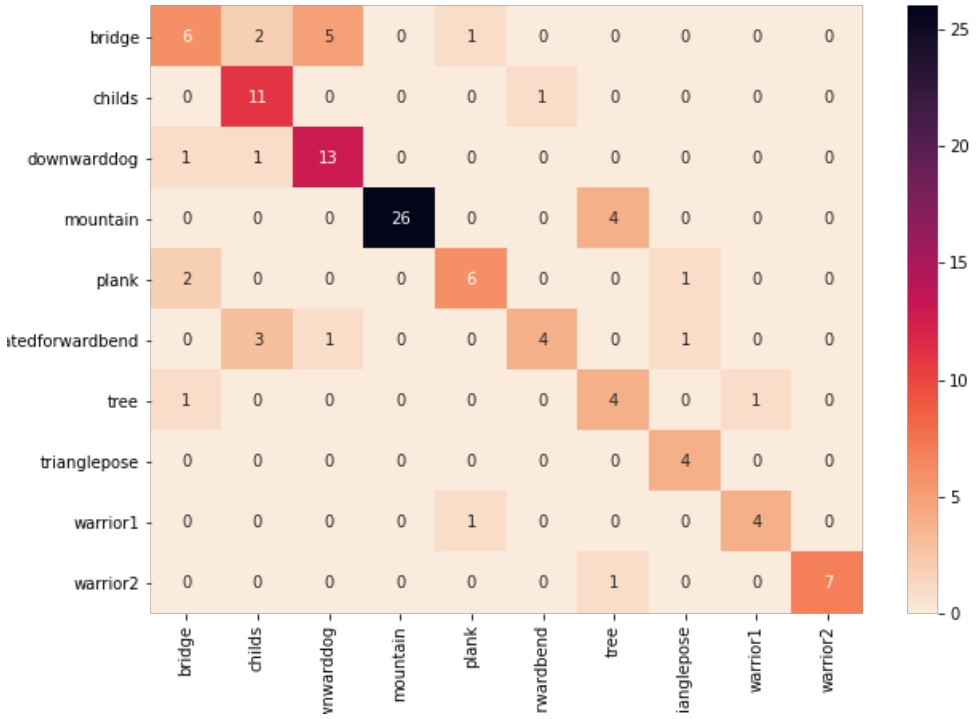

(b) Using proportions.

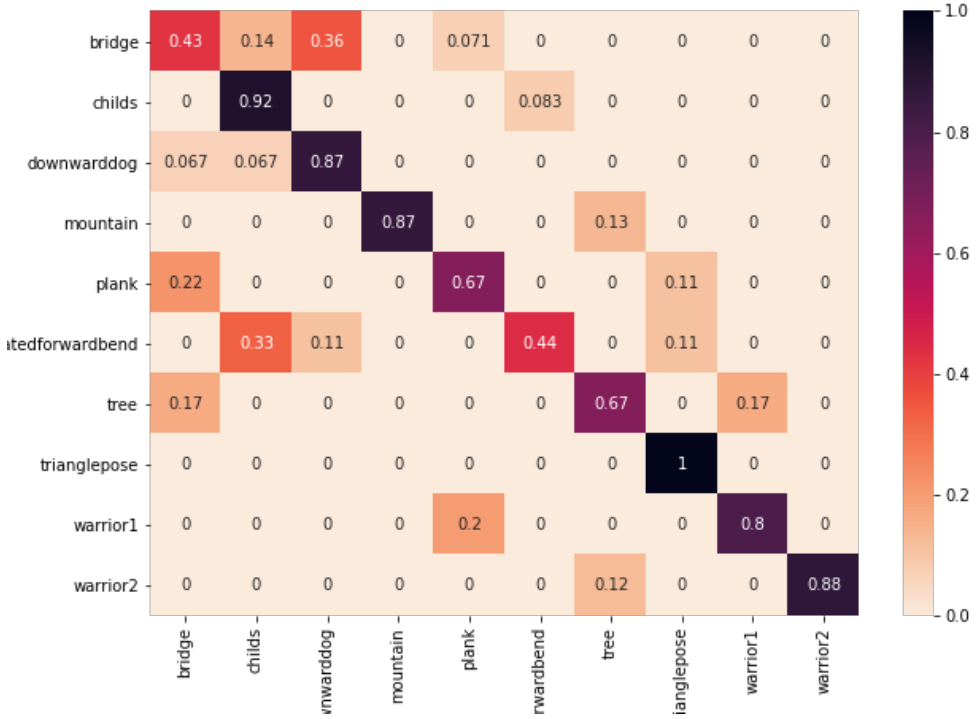

Question 2: Gaussian Distribution Assumption

The Gaussian Naïve Bayes classifier assumes that observations for attributes are normally distributed within each class. To check the validity of these assumptions a large amount of visualisations were generated, the most useful of which are presented below.

The number of normal distributions that are fit for the Gaussian Naïve Bayes classifier is equal to the number of classes (10) times the number of attributes (22). To exhaustively check the normal assumption would be to verify it held for all of these 220 distributions. It does not.

This was visualised in two ways, the prettiest and most information dense option being a scatterplot of the coordinates of a body part for all of the different poses. Marginal density plots on each of the axes allow us to assess the distribution of coordinates for each axis, for each pose. These plots for each of the body parts are shown in figure 3 from appendix B, but we will look specifically at figures 3a and 3b for an example. These will be used to argue that there is insufficient evidence in this data to conclude that violating the assumption of normality decreases the accuracy of classification results.

Firstly, it can be observed from figure 1b that Triangle pose was the class most accurately classified by the model, and Bridge pose was the least. Looking closely it can be seen in the marginal density plots on figures 3a and 3b that the Triangle pose does not fit well to a Gaussian distribution, and Bridge pose does significantly better, especially in the distribution of the x coordinates, where Triangle pose seems to be multimodal (which is not a property of normal distributions). We can visualise this more clearly by taking Normal QQ plots of these body part coordinates. This is shown in appendix A figure 2, where 2a and 2b show convincingly that these data points from the Triangle pose data do *not* follow a normal distribution. Figures 2c and 2d show that the Bridge pose coordinates do fit the normal distribution better, though still not perfectly.

Because the class most accurately predicted by the model shows less adherence to the normal assumption than the class worst predicted in many of the cases, there is insufficient evidence to conclude that violation of the normal assumption has a negative effect on the accuracies of the classifiers predictions.

Appendices

A Normal QQ Plots of Body Part Coordinate Distributions

Figure 2: A visualisation of two confusion matrices for the model's classification of the testing data.

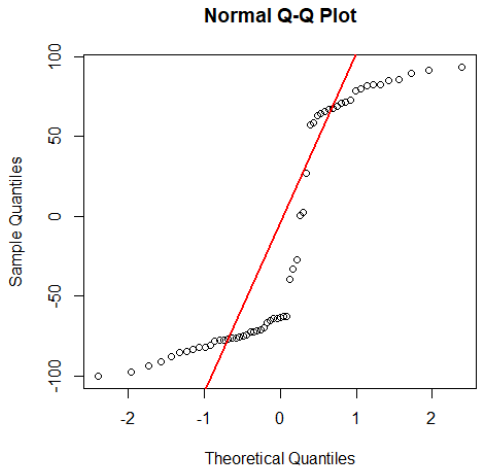

(a) QQ Plot for x coordinates of heads from Triangle poses.

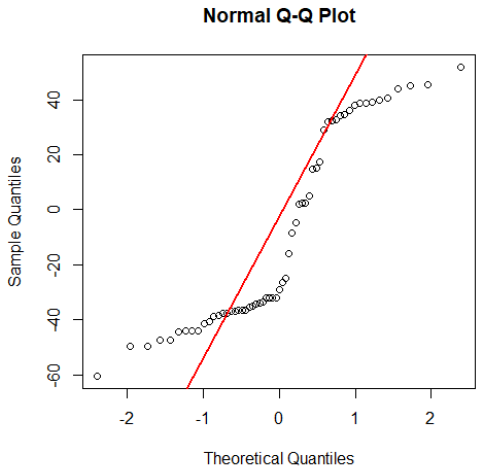

(b) QQ Plot for x coordinates of chests from Triangle poses.

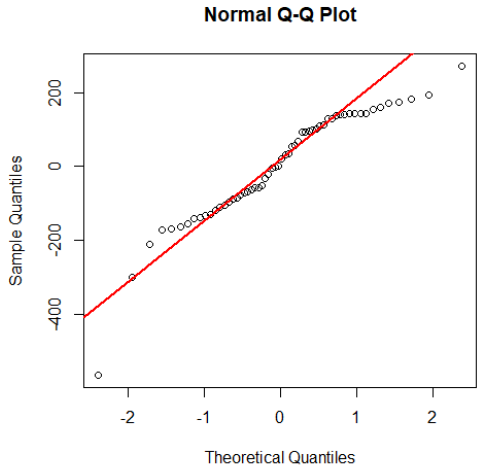

(c) QQ Plot for x coordinates of heads from Bridge poses.

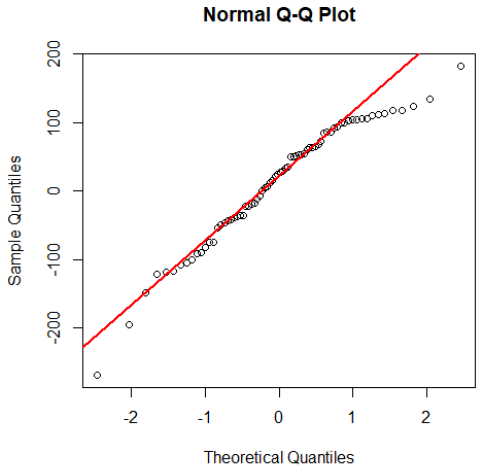

(d) QQ Plot for x coordinates of chests from Bridge poses.

B Body Part Distribution Scatterplots

Figure 3: Scatterplots of all body part coordinates in training data with marginal distributions. Coloured by true pose. (You can ignore most of these, they are just included for completeness and because they look nice :))

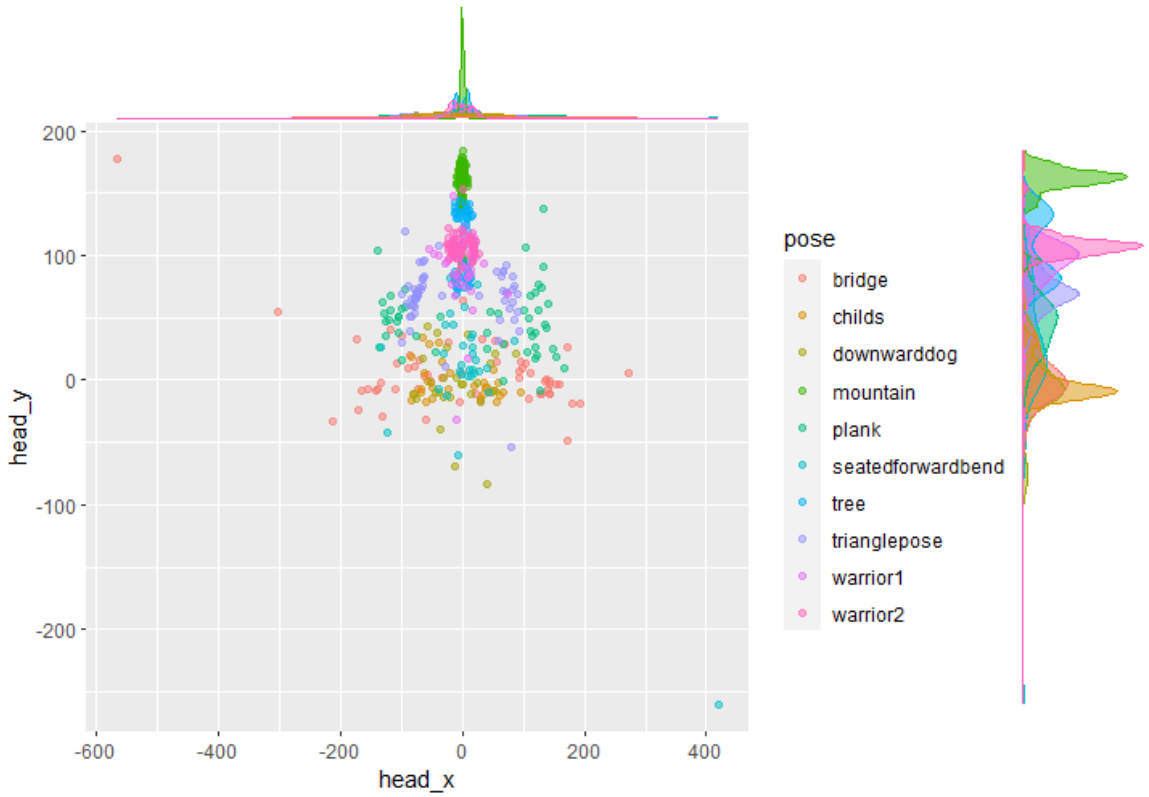

(a) The distribution of head coordinates with marginal density plots.

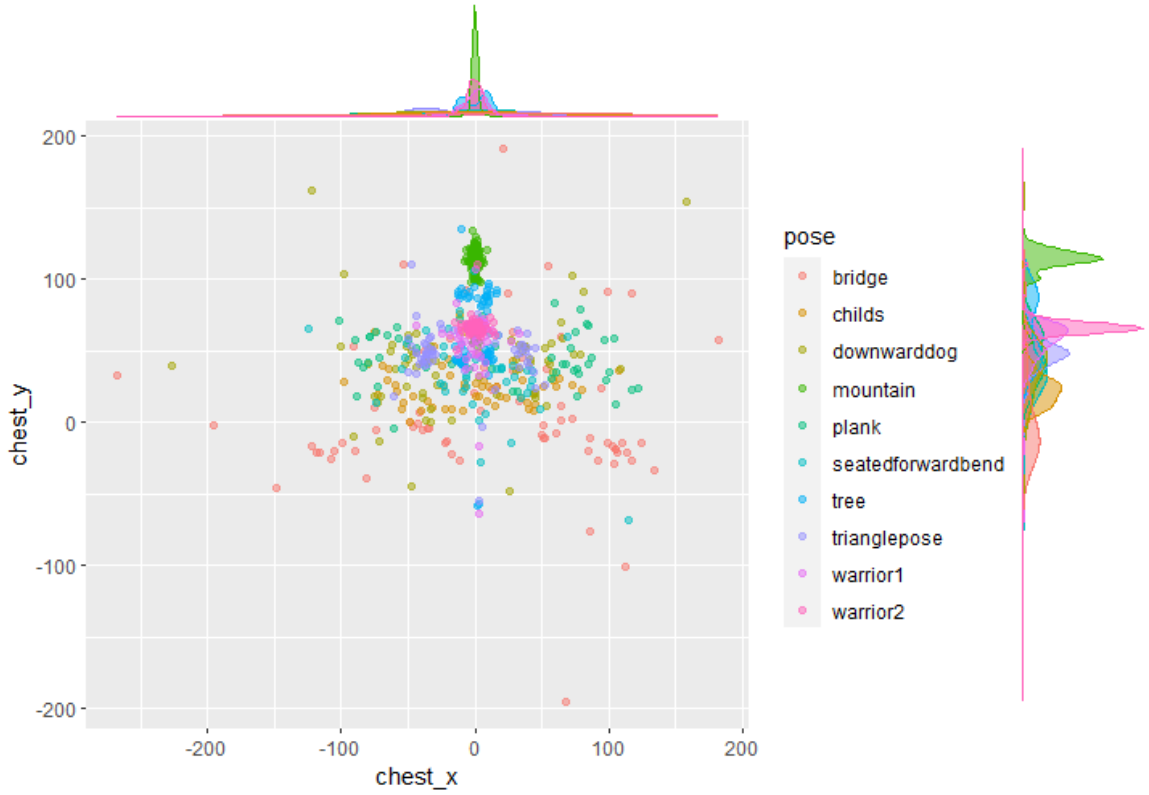

(b) The distribution of chest coordinates with marginal density plots.

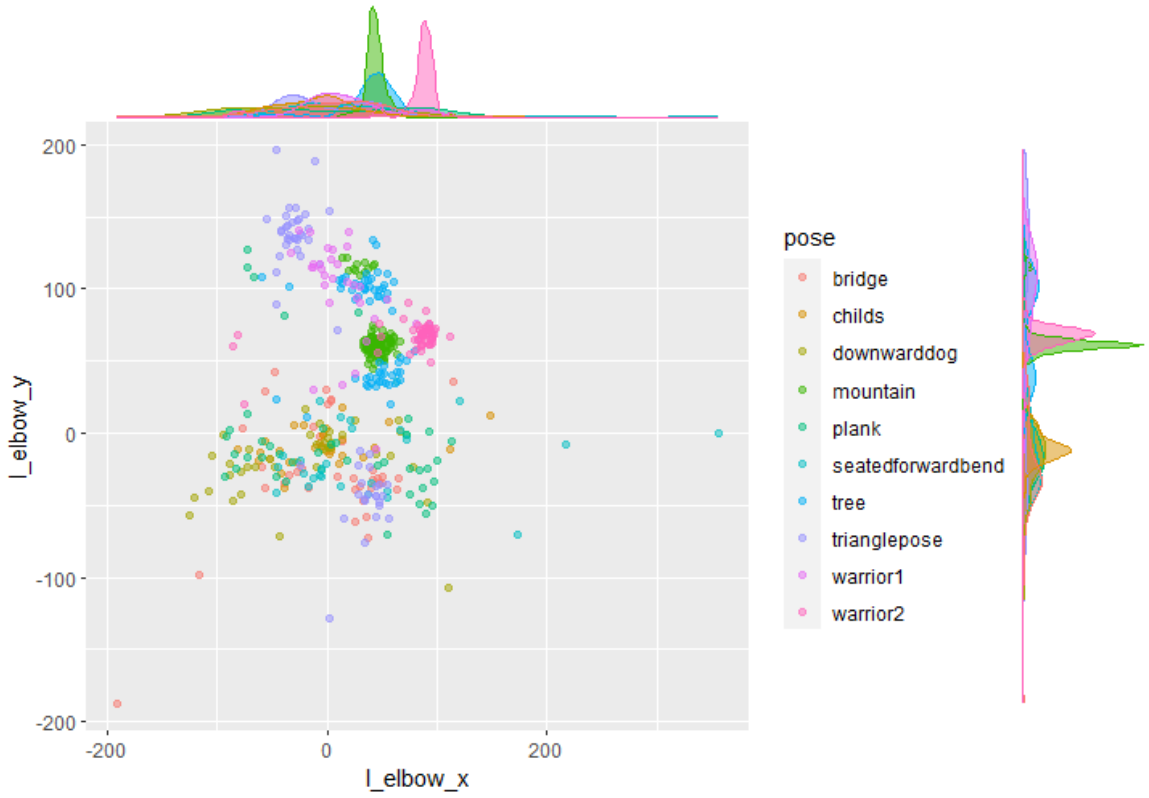

(c) The distribution of left elbow coordinates with marginal density plots.

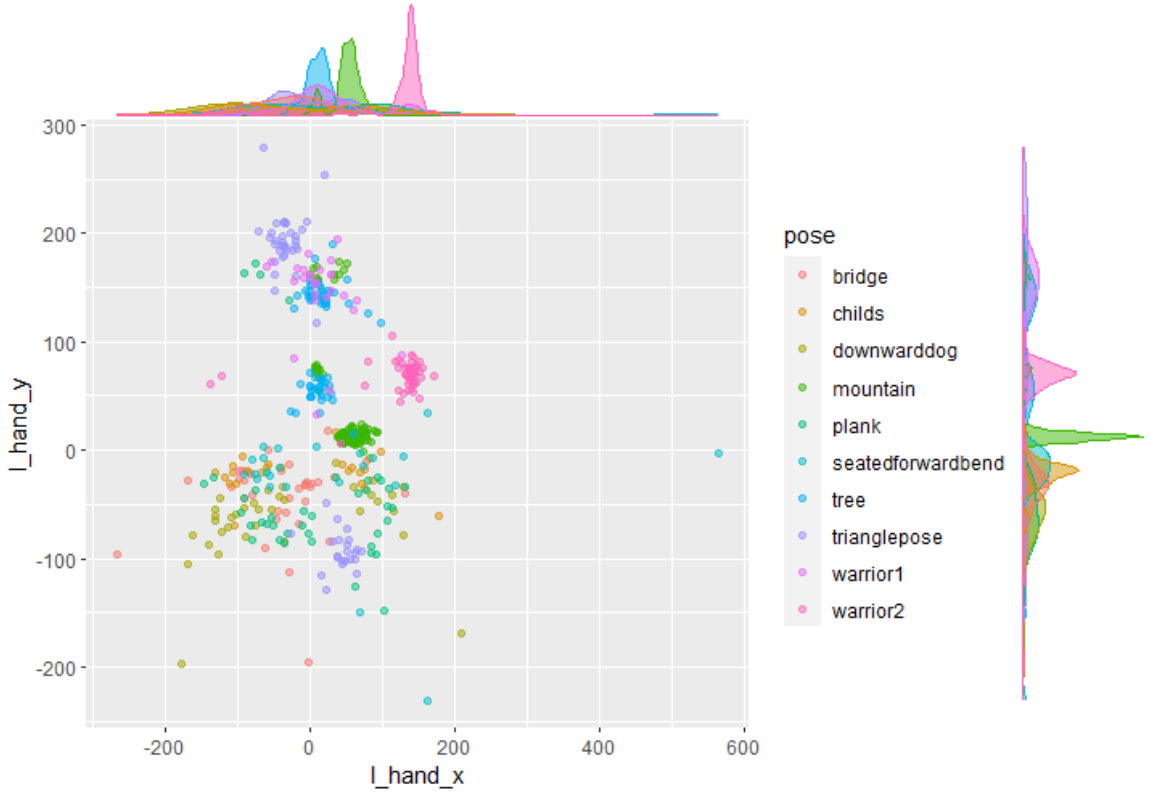

(d) The distribution of left hand coordinates with marginal density plots.

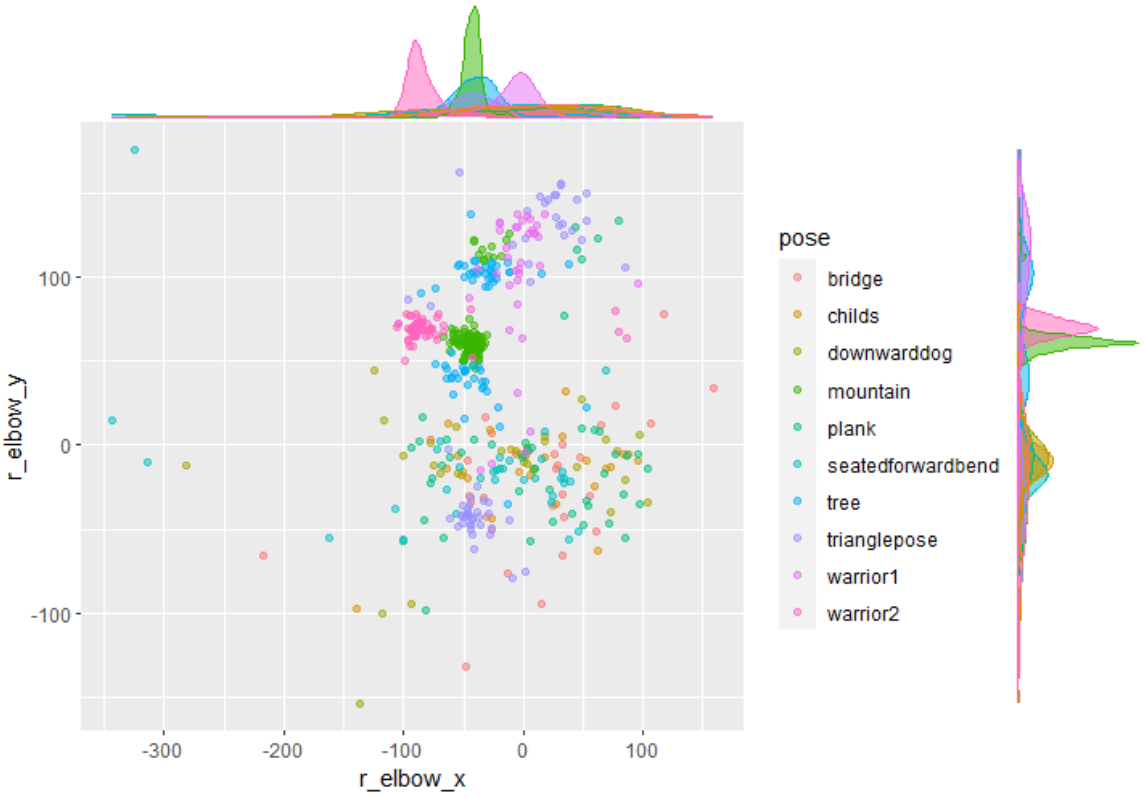

(e) The distribution of right elbow coordinates with marginal density plots.

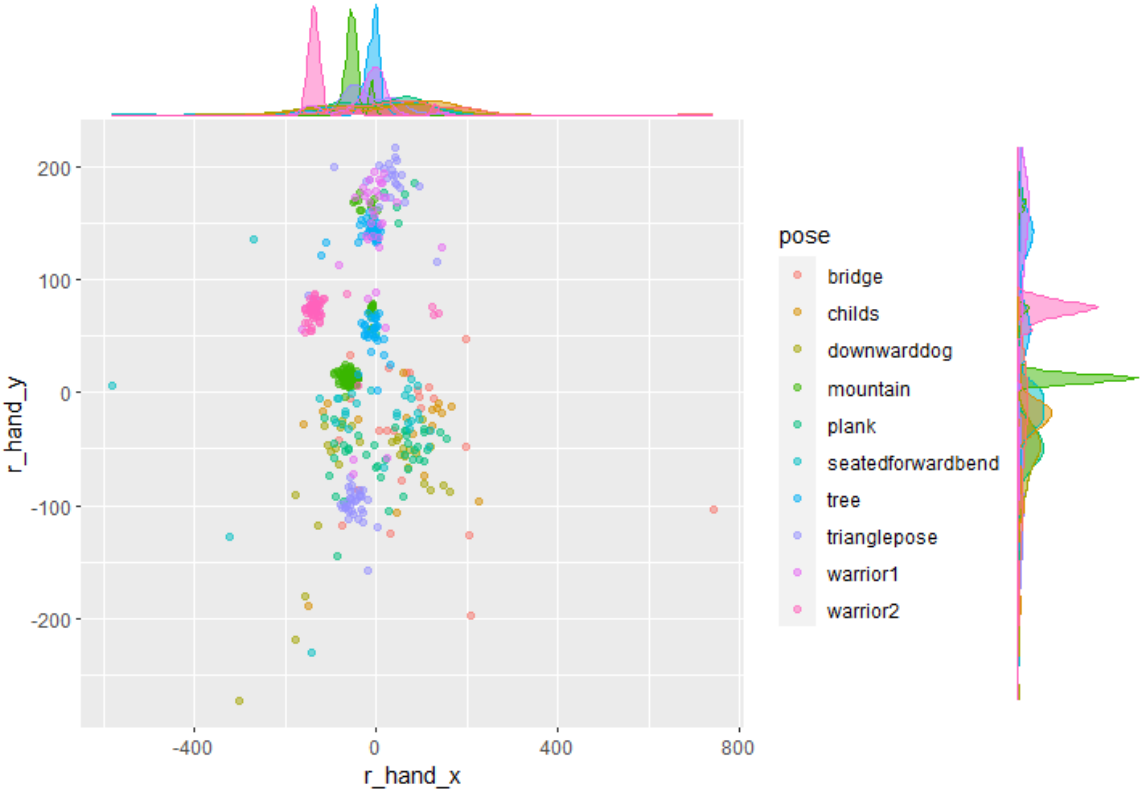

(f) The distribution of right hand coordinates with marginal density plots.

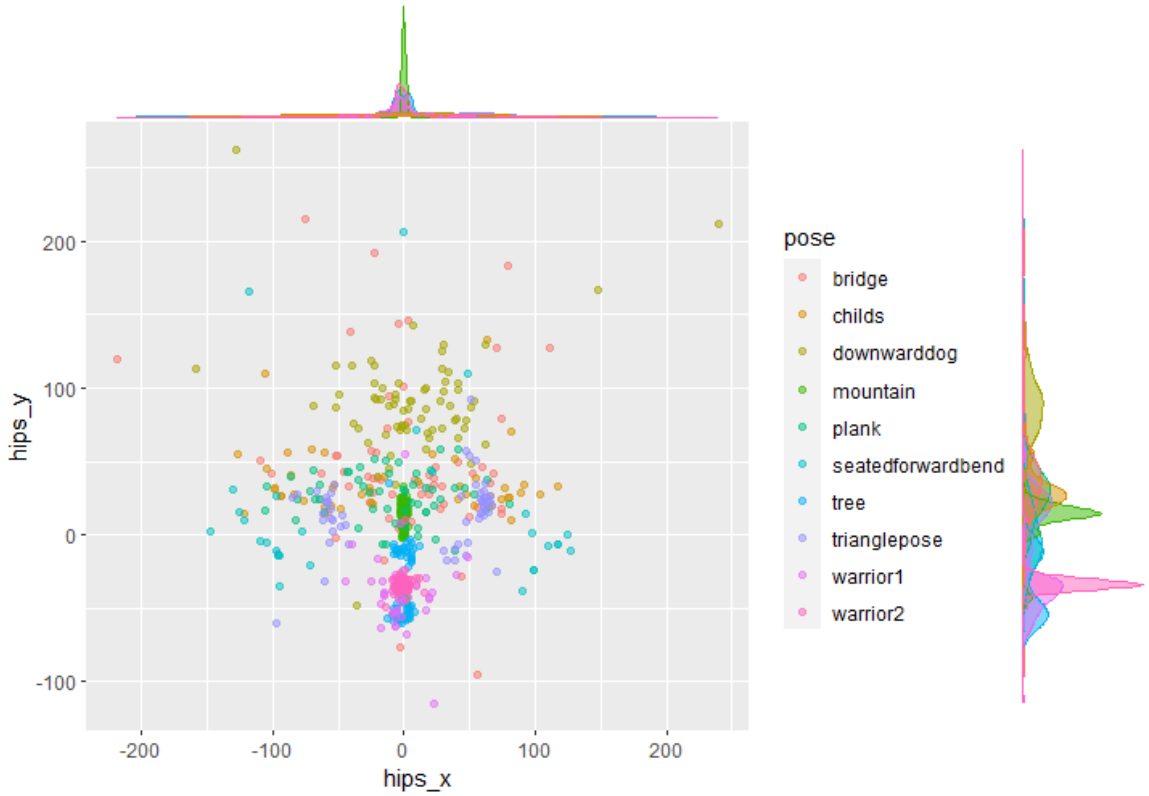

(g) The distribution of hip coordinates with marginal density plots.

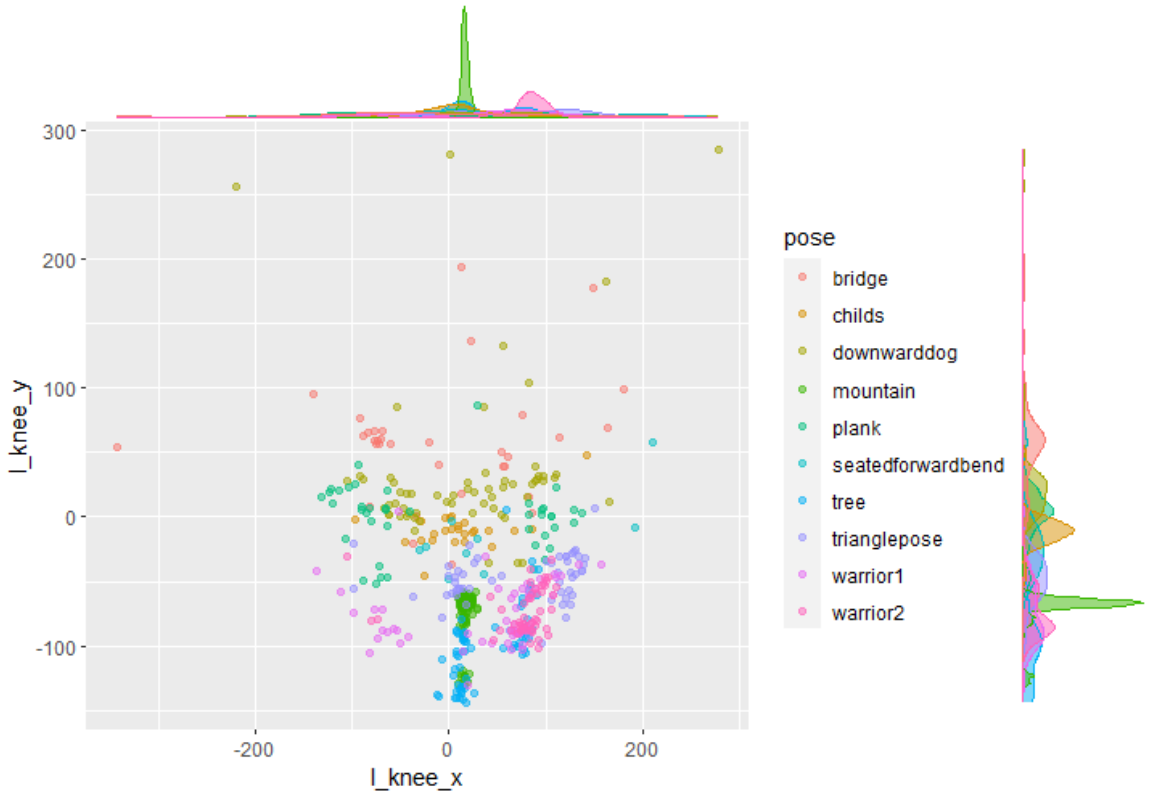

(h) The distribution of left knee coordinates with marginal density plots.

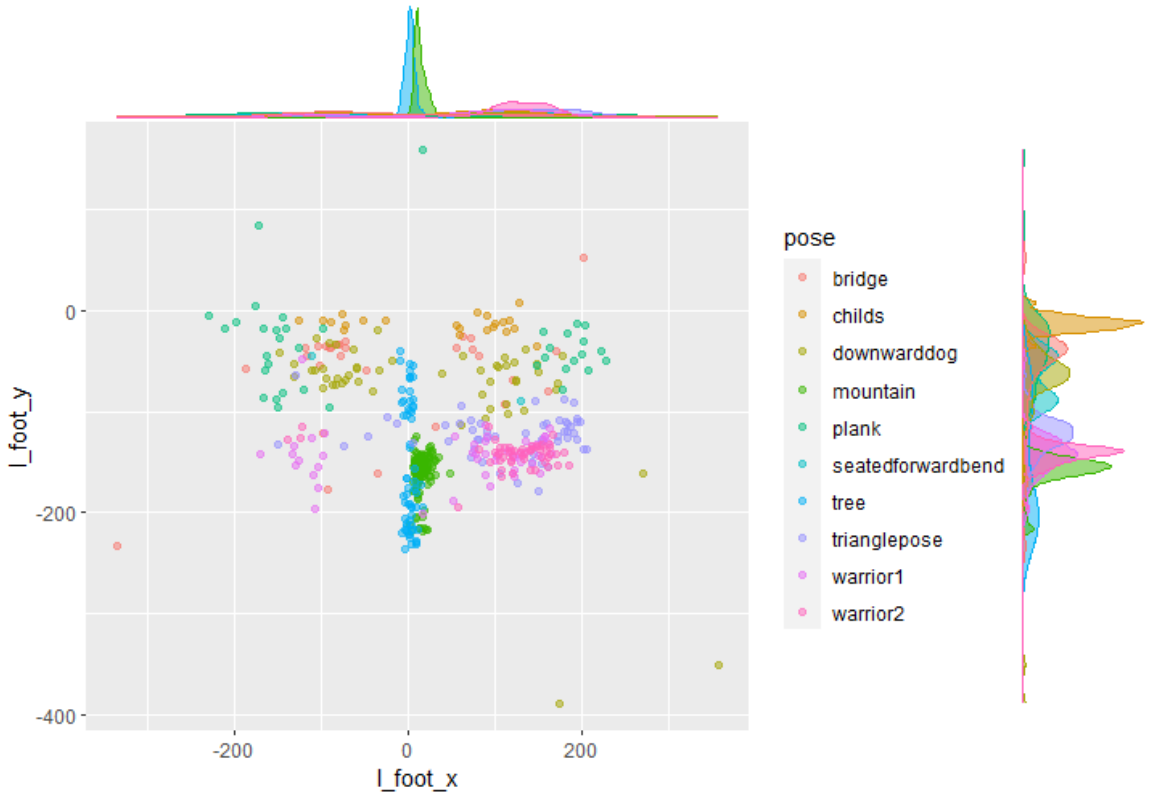

(i) The distribution of left foot coordinates with marginal density plots.

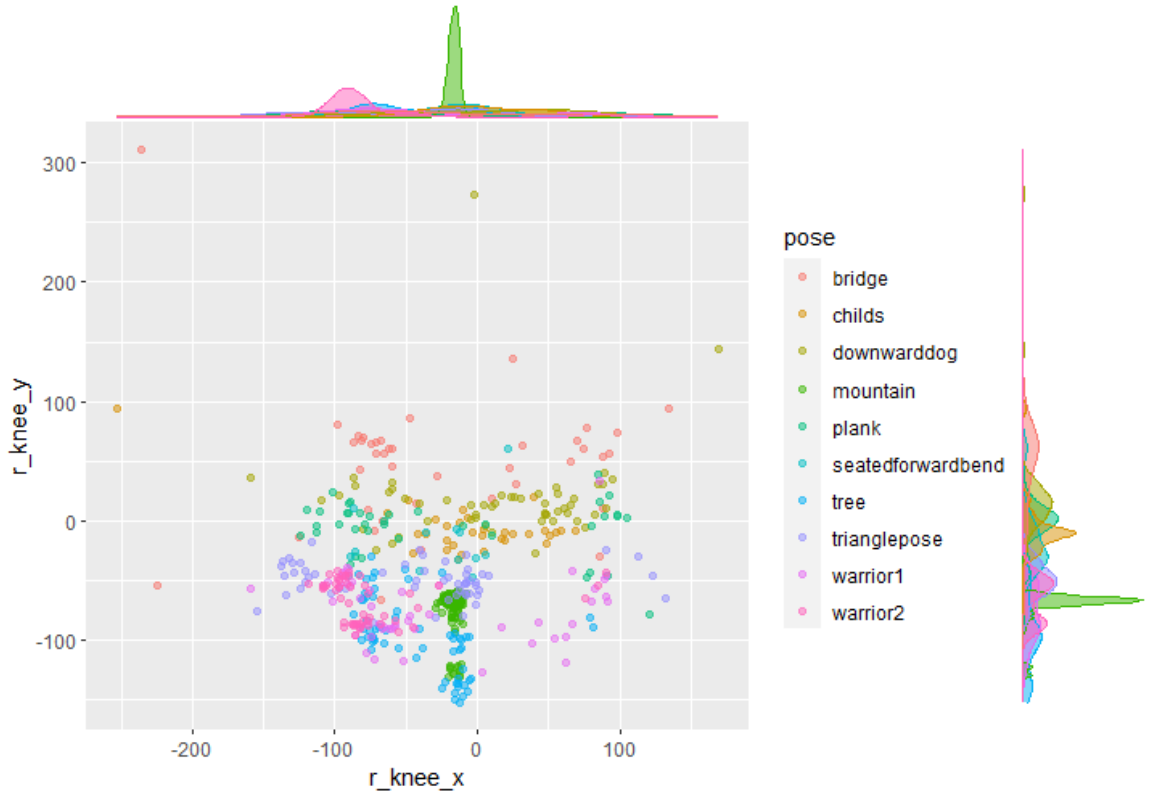

(j) The distribution of right knee coordinates with marginal density plots.

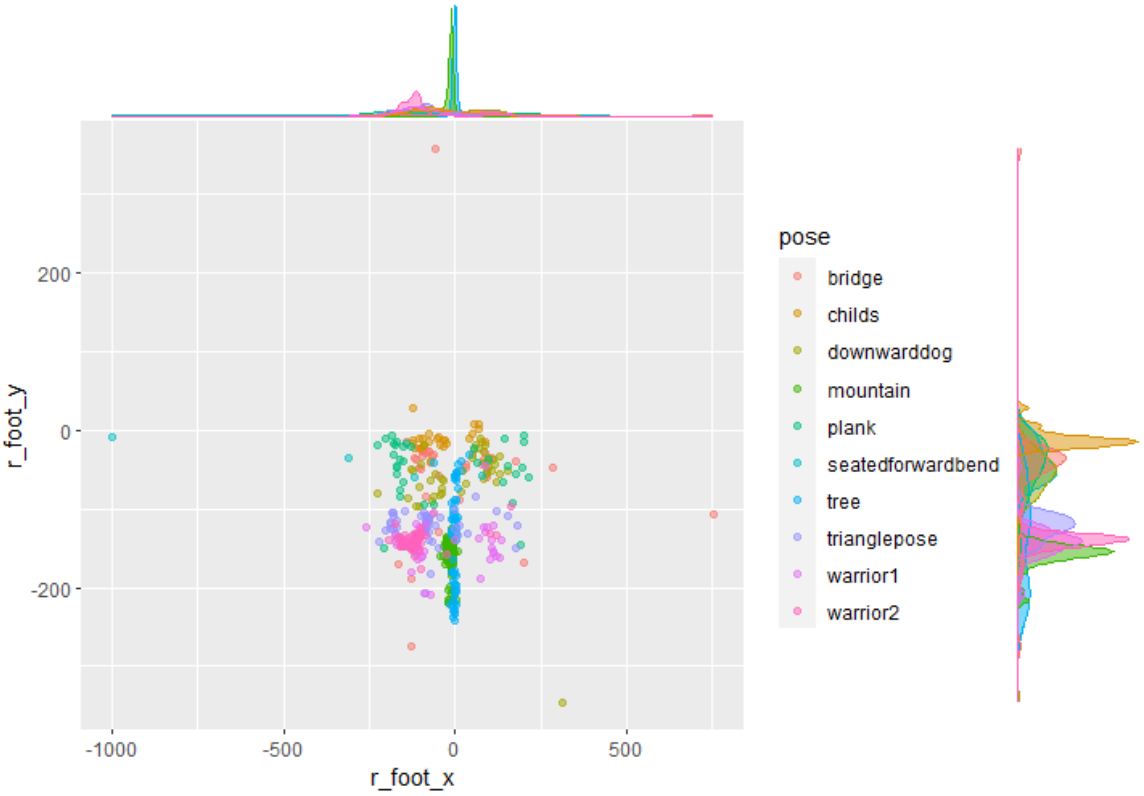

(k) The distribution of right foot coordinates with marginal density plots.